IEEE Photonics Journal
An IEEE Photonics Society Publication

Open Access

Minimization of Feedback Loop Distortions in Digital Predistortion of a Radio-Over-Fiber System With Optimization Algorithms

Volume 9, Number 3, June 2017

Carlos Mateo, ***Student Member, IEEE***
Pedro L. Carro, ***Member, IEEE***
Paloma García-Dúcar
Jesús de Mingo
Íñigo Salinas

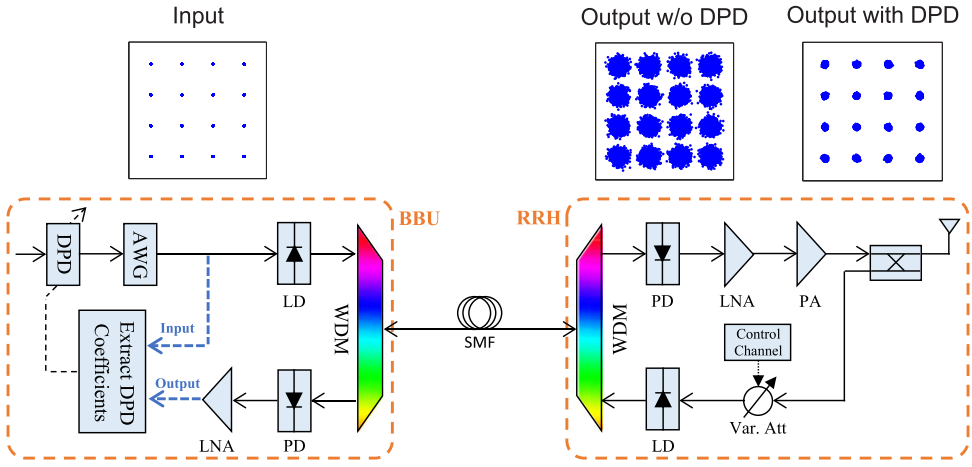

DOI: 10.1109/JPHOT.2017.2706364
1943-0655 © 2017 IEEE

IEEE photonics SOCIETY

IEEE

Minimization of Feedback Loop Distortions in Digital Predistortion of a Radio-Over-Fiber System With Optimization Algorithms

Carlos Mateo, *Student Member, IEEE*, Pedro L. Carro, *Member, IEEE*, Paloma García-Dúcar, Jesús de Mingo, and Íñigo Salinas

Department of Electronic Engineering and Communications Aragon Institute of Engineering Research (I3A), University of Zaragoza, Zaragoza 50.018, Spain

DOI:10.1109/JPHOT.2017.2706364
1943-0655 © 2017 IEEE. Translations and content mining are permitted for academic research only. Personal use is also permitted, but republication/redistribution requires IEEE permission. See http://www.ieee.org/publications_standards/publications/rights/index.html for more information.

Manuscript received April 18, 2017; revised May 15, 2017; accepted May 16, 2017. Date of publication May 23, 2017; date of current version June 1, 2017. This work was supported by Spanish MINECO (TEC2014-58341-C4-2-R within FEDER) and Diputación General de Aragón (GCM T97). Corresponding author: Carlos Mateo (e-mail: cmperez@unizar.es).

Abstract: This article proposes the linearization of an intensity modulation/direct detection radio-over-fiber (RoF) link with feedback loop. The goal is to carry out the predistortion process in a real scenario, in which the output signals are a few kilometers far from the baseband unit (BBU). First, the feedback loop is considered ideal, so the output signals are captured at the remote radio head side. Then, the feedback loop is taken into account, and both the input and output signals are captured at the BBU side. Applying optimization algorithms, such as Fibonacci, Golden, or Powell, it is possible to seek the optimal attenuation value within only a few iterations, which minimizes the distortion of the feedback loop. Experiments are carried out in a RoF system with 10 and 25 km length fiber within the long-term evolution (LTE) standard. Measured results show how with a proper choice of the attenuation it is possible to reach analogous results regarding to an ideal feedback loop in terms of adjacent channel power ratio, the output signal power and error vector magnitude.

Index Terms: CPWL models, Digital Predistortion (DPD), Feedback Loop, Linearization, Long Term Evolution (LTE), Radio-over-Fiber (RoF).

1. Introduction

Currently, new architectures have been developed in order to support the increasing demand for broadband wireless access, such as Cloud Radio Access Network (C-RAN) [1]–[4]. It consists of a centralized baseband unit (BBU) with several remote radio heads (RRHs). Radio-over-Fiber (RoF) systems have been proposed as an alternative for connecting the BBU with the RRHs, due to the fact that these links provide a strong cost-effective solution to improve the system capacity of wireless links. Furthermore, optical fiber links offer benefits, such as extremely broad bandwidth, immunity to electromagnetic interferences and the signals can be sent through larger transmission distances with a low loss of power [5], [6]. One main drawback of these systems is that the signals may suffer distortions from the electrical-to-optical (OE) and electrical-to-optical (EO) conversions or the fiber dispersion [7]. Since the power amplifier (PA) situated at the RRH side is working in its saturation region in order to increase its power efficiency, it can also distort the signals [8].

All of these effects produce a spectral regrowth in adjacent bands. Nowadays, several modulation schemes with high-spectral efficiency, like orthogonal frequency division multiplexing (OFDM), are used in current standards such as Long Term Evolution (LTE) [9]. One main drawback that presents these signals is their high peak-to-average power ratio (PAPR) in their signal envelopes [10]. When the PAPR is high, the RoF system will require high linearity.

Along the literature, several photonic techniques have been developed, such as dual wavelength linearization or mixed polarization [11]–[13], but the system complexity may be increased. Digital predistortion (DPD) is one of the widely used techniques to improve the system linearity. The advantages of DPD include its low-cost, high-robustness, and good performance reducing the intermodulation products. The canonical piecewise-linear function (CPWL) was introduced by Chua [14] in 1977, and then modified using a decomposed vector rotation technique and applied in a PA linearization process [15]. The DPD based on CPWL functions is applied in an intensity modulated/direct detection (IM/DD) RoF system in [16], where it is demonstrated that CPWL models offer better performance regarding to classical Volterra models. The main disadvantage in the linearization process of a RoF link is that the output signals may be a few kilometers far from the BBU, so it is necessary to feedback these signals from the RRH to the BBU. Until now, predistorter models which are applied to a RoF mobile fronthaul systems have considered the feedback link as ideal, capturing the output signals at the RRH side. However, in real systems these signals have to be sent back through the feedback RoF system, so these signals will be affected by the E/O and O/E conversions, as well as the fiber dispersion.

In this work we propose the use of a feedback loop using the same fiber link, sending the downlink and feedback signals with different wavelengths (WDM). Applying optimization algorithms, such as Fibonacci, Golden or Powell, it is possible to seek the optimal attenuation at the feedback RoF input within only a few iterations, which minimizes the distortion of the feedback loop. Experiments are carried out in a RoF mobile fronthaul link with 10 and 25 km-length fiber within the Band 7 of the LTE standard. Experimental results show that with a suitable choice of the attenuation it is possible to reach analogous results regarding to the ideal case in terms of adjacent channel power ratio (ACPR), output signal power and error vector magnitude (EVM).

This article is organized as follows. Section 2 presents the proposed model. Optimization algorithms are stated in Section 3. The linearization process in an ideal scenario is shown in Section 4. Section 5 presents the experimental results with the feedback loop in the setup, and finally, Section 6 contains the conclusions.

2. Predistorter Model

The predistorter model used in this work is based on the CPWL functions proposed in [11]. Balancing the performance and the implementation complexity, a truncated version of this model has been used, taking into account only up to 2nd-order type-2, in order to minimize the coefficient number. This model is defined as

$$\begin{aligned} x_{BBU}^{PD}(n) = & \sum_{m=0}^{M} \pi_m x_{BBU}(n-m) \\ & + \sum_{k=1}^{K} \sum_{m=0}^{M} \pi_{km,1} \left| \left| x_{BBU}(n-m) \right| - \beta_k \right| e^{j\theta(n-m)} \\ & + \sum_{k=1}^{K} \sum_{m=0}^{M} \pi_{km,21} \left| \left| x_{BBU}(n-m) \right| - \beta_k \right| e^{j\theta(n-m)} \cdot \left| x_{BBU}(n) \right| \\ & + \sum_{k=1}^{K} \sum_{m=0}^{M} \pi_{km,22} \left| \left| x_{BBU}(n-m) \right| - \beta_k \right| \cdot x_{BBU}(n), \end{aligned} \tag{1}$$

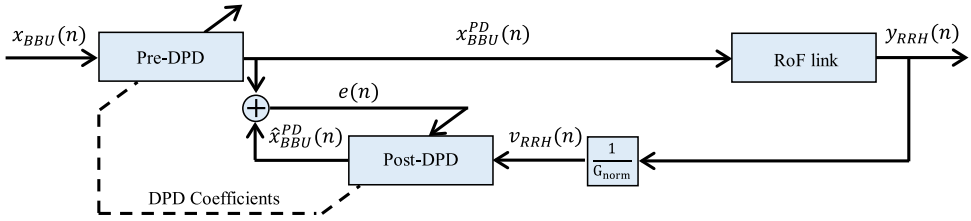

Fig. 1. Experimental setup for a RoF mobile fronthaul system with ideal feedback loop.

where K is the number of partitions and M represents the memory depth. β_k is the threshold that defines the boundary of the partition, defined as $\beta_k = \left|x_{BBU_{\max}}\right| \cdot k/K$. $x_{BBU}(n)$ and $x_{BBU}^{PD}(n)$ are the predistorter baseband input and output signals, respectively. On the other hand, π_m, $\pi_{km,1}$, $\pi_{km,21}$ and $\pi_{km,22}$ are the coefficient vectors. The predistorter scheme using indirect learning structure appears in Fig. 1. DPD coefficients are computed in a first training stage in the feedback path, whose input is the normalized RoF output sequence $v_{RRH}(n)$, defined as $v_{RRH}(n) = y_{RRH}(n)/G_{norm}$, with G_{norm} the complex gain of the whole system. There are different approaches for estimating the model coefficients when applying DPD. When the dependence of the coefficients regarding the input samples is linear, least squares (LS) algorithms can be applied [17]. The predistorter coefficients are obtained by means of the least squares minimization, whose solution is the pseudoinverse of the normalized DPD output $x_{BBU}^{PD}(n)$. The coefficient vector can be obtained according to the following expression

$$\hat{\pi} = (V_{RRH}{}^{H} V_{RRH})^{-1} V_{RRH}{}^{H} x_{BBU}, \tag{2}$$

where $\hat{\pi}$ represents the DPD coefficient vector and $(V_{RRH}{}^{H} V_{RRH})^{-1} V_{RRH}{}^{H}$ the pseudoinverse of V_{RRH}, which is defined as

$$V_{RRH} = \begin{pmatrix} v(n)_{m}^{RRH} & v(n)_{1m,1}^{RRH} & \cdots & v(n)_{Km,22}^{RRH} \\ v(n+1)_{m}^{RRH} & v(n+1)_{1m,1}^{RRH} & \cdots & v(n+1)_{Km,22}^{RRH} \\ \vdots & \vdots & \ddots & \vdots \\ v(n+T-1)_{m}^{RRH} & v(n+T-1)_{1m,1}^{RRH} & \cdots & v(n+T-1)_{Km,22}^{RRH} \end{pmatrix}, \tag{3}$$

with T the length of $v_{RRH}(n)$. The matrix terms are

$$v(n)_{m}^{RRH} = v_{RRH}(n-m) \tag{4}$$

$$v(n)_{km,1}^{RRH} = \left| \left|v_{RRH}(n-m)\right| - \frac{\left|v_{RRH_{\max}}\right| \cdot k}{K} \right| e^{j\theta(n-m)}, \tag{5}$$

$$v(n)_{km,21}^{RRH} = \left| \left|v_{RRH}(n-m)\right| - \frac{\left|v_{RRH_{\max}}\right| \cdot k}{K} \right| e^{j\theta(n-m)} \cdot \left|v_{RRH}(n-m)\right|, \tag{6}$$

$$v(n)_{km,22}^{RRH} = \left| \left|v_{RRH}(n-m)\right| - \frac{\left|v_{RRH_{\max}}\right| \cdot k}{K} \right| \cdot v_{RRH}(n-m). \tag{7}$$

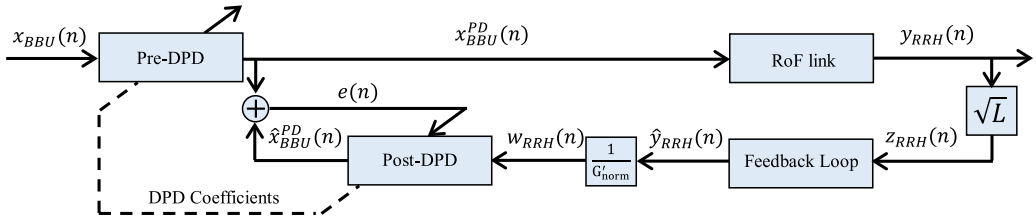

Fig. 2. Experimental setup for a RoF mobile fronthaul system with feedback loop.

When the feedback loop is taken into account (see Fig. 2) and is modeled using the same plant as Eq. (1) (but different coefficients denoted as λ), the received signal at the BBU side is defined as

$$\begin{aligned}\hat{y}_{RRH}(n) = &\sum_{m=0}^{M} \lambda_m z_{RRH}(n-m) \\ &+ \sum_{k=1}^{K}\sum_{m=0}^{M} \lambda_{km,1} \left| |z_{RRH}(n-m)| - \frac{|z_{RRH_{\max}}| \cdot k}{K} \right| e^{j\theta(n-m)} \\ &+ \sum_{k=1}^{K}\sum_{m=0}^{M} \lambda_{km,21} \left| |z_{RRH}(n-m)| - \frac{|z_{RRH_{\max}}| \cdot k}{K} \right| e^{j\theta(n-m)} \cdot |z_{RRH}(n)| \\ &+ \sum_{k=1}^{K}\sum_{m=0}^{M} \lambda_{km,22} \left| |z_{RRH}(n-m)| - \frac{|z_{RRH_{\max}}| \cdot k}{K} \right| \cdot z_{RRH}(n), \end{aligned} \tag{8}$$

where $z_{RRH}(n)$ is defined as $z_{RRH}(n) = y_{RRH}(n)/\sqrt{L}$, with $\sqrt{L}$ the envelope attenuation at the beginning of the feedback loop. If we assume that $\sqrt{L}$ is set at its optimum value and the feedback loop operates in its linear region, the received signal can be safely approximated as

$$\hat{y}_{RRH}(n) \simeq \sum_{m=0}^{M} \lambda_m \frac{y_{RRH}(n-m)}{\sqrt{L}} + \sum_{k=1}^{K}\sum_{m=0}^{M} \lambda_{km,1} \left| \left| \frac{y_{RRH}(n-m)}{\sqrt{L}} \right| - \frac{|y_{RRH_{\max}}| \cdot k}{\left|\sqrt{L}\right| \cdot K} \right| \cdot e^{j\theta(n-m)}, \tag{9}$$

and thus the second term can be approximated with a linear expression. Moreover, if we consider that the memory effects are negligible, the received signal can be defined as

$$\begin{aligned}\hat{y}_{RRH}(n) &\simeq \frac{y_{RRH}(n)}{\sqrt{L}} + \xi(\lambda_{1,} \cdots \lambda_K) \cdot \left| \frac{y_{RRH}(n)}{\sqrt{L}} \right| \cdot e^{j\theta(n)} \\ &= \underbrace{\left(\frac{1}{\sqrt{L}} + \frac{\xi(\lambda_{1,} \cdots \lambda_K)}{\left|\sqrt{L}\right|} \right)}_{\Delta} \cdot y_{RRH}(n), \end{aligned} \tag{10}$$

where $\xi(\lambda_{1,} \cdots \lambda_K)$ is a linear expression which depends of the model coefficients and Δ represents the attenuation effects produced by the attenuator of the feedback loop. Now, the postdistorter input signal is $w_{RRH}(n)$, defined as $w_{RRH}(n) = \hat{y}_{RRH}/G'_{norm}$, where G'_{norm} is the normalized gain of the whole system. Thus, the coefficient vector of the whole system is:

$$\hat{\mathrm{w}}_{\pi} = (\mathrm{W_{RRH}}^{H} \mathrm{W_{RRH}})^{-1} \mathrm{W_{RRH}}^{H} \mathrm{x_{BBU}}, \tag{11}$$

with W_{RRH} defined as

$$W_{RRH} = \begin{pmatrix} w(n)_{m}^{RRH} & w(n)_{1m,1}^{RRH} & \cdots & w(n)_{Km,22}^{RRH} \\ w(n+1)_{m}^{RRH} & w(n+1)_{1m,1}^{RRH} & \cdots & w(n+1)_{Km,22}^{RRH} \\ \vdots & \vdots & \ddots & \vdots \\ w(n+T-1)_{m}^{RRH} & w(n+T-1)_{1m,1}^{RRH} & \cdots & w(n+T-1)_{Km,22}^{RRH} \end{pmatrix}. \tag{12}$$

with T the length of $w_{RRH}(n)$. The first matrix element $w(n)_{m}^{RRH}$ is defined as

$$w(n)_{m}^{RRH} = w_{RRH}(n-m) = \Delta \cdot v_{RRH}(n-m) = \Delta \cdot v(n)_{m}^{RRH}. \tag{13}$$

Operating in the same way, the rest of coefficients can be obtained as

$$w(n)_{km,1}^{RRH} = |\Delta| \cdot v(n)_{km,1}^{RRH}, \tag{14}$$

$$w(n)_{km,21}^{RRH} = |\Delta|^2 \cdot v(n)_{km,21}^{RRH}, \tag{15}$$

$$w(n)_{km,22}^{RRH} = |\Delta| \cdot \Delta \cdot v(n)_{km,22}^{RRH}. \tag{16}$$

The matrix W_{RRH} can be expressed as $W_{RRH} = L_{RRH} \cdot V_{RRH}$, with L_{RRH} the attenuation matrix defined as

$$L_{RRH} = \begin{pmatrix} \Delta & 0 & \cdots & 0 \\ 0 & |\Delta| & \cdots & 0 \\ \vdots & \vdots & \ddots & \vdots \\ 0 & 0 & \cdots & |\Delta| \cdot \Delta \end{pmatrix}. \tag{17}$$

Substituying in Eq. (11), the coefficient vector can be obtained according to the following equation

$$\hat{w}_{\pi} = \left[(L_{RRH} \cdot V_{RRH})^{H} \cdot L_{RRH} \cdot V_{RRH} \right]^{1} (L_{RRH} \cdot V_{RRH})^{H} \cdot x_{BBU}. \tag{18}$$

Applying basic linear algebra rules,

$$\hat{w}_{\pi} = L_{RRH}^{-1} \cdot \left(V_{RRH}^{H} \cdot V_{RRH} \right)^{-1} \cdot V_{RRH}^{H} \cdot x_{BBU} = L_{BBU}^{-1} \cdot \hat{\pi}, \tag{19}$$

which demonstrates that it is necessary to compensate the receiver signal power with the attenuation matrix. This result shows that the new coefficient vector is essentially a scaled version of the ideal estimation and justifies that the DPD estimation can be improved by selecting a feasible attenuation at the RRH side.

3. Optimization Algorithms

In order to feedback the output signals as linear as possible, it is necessary to set properly the input signal power at the feedback chain input. This issue is carried out by means of a variable attenuator, whose value will influence on the output signal distortion. We propose the use of several optimization algorithms in order to seek the optimal attenuation (L_{opt}), reducing the number of iterations. If we define the EVM of the received signals as φ, the optimization process yields to an optimum attenuation which fulfills:

$$L_{opt} = \arg\min \{ \varphi(L) \} \tag{20}$$

A method for seeking the minimum of $\varphi(L)$ is to evaluate the function many times and search for a minimum. If we take into account that the demodulation process is the most time-consuming part in the optimization process, it is important to reduce the number of function evaluations. There are different algorithms which after several iterations converge to the optimal solution. In this work we propose the use of unconstrained optimization techniques, such as *Fibonacci*, *Golden Ratio* and *Powell*. In order to apply these methods the $\varphi(L)$ must be unimodal over the interval $[L_1^{(k)}, L_2^{(k)}]$, and has to have an unique minimum.

3.1 Fibonacci

The Fibonacci search [18] is based on the sequence of Fibonacci numbers $\{F_k\}_{k=0}^{\infty}$ defined by the equations: $F_0 = 0$, $F_1 = 1$ and $F_n = F_{n-1} + F_{n-2}$, for $n = 2, 3, \cdots$. The Fibonacci search can be inicialized with $r_0 = F_{n-1}/F_n$, with r_0 a value so that both of the interior points $L_3^{(1)}$ and $L_4^{(1)}$ will be used in the next subinterval and there will be only one new function evaluation. Then it continues by using $r_k = F_{n-1-k}/F_{n-k}$ for $k = 1, 2, \cdots, n-3$. The $(k+1)$st subinterval is obtained by reducing the length of the kth subinterval by a factor of $r_k = F_{n-1-k}/F_{n-k}$. If the abscissa of the minimum is to be found with a precision of ε, we need to find the smallest value of n such that

$$F_n > \frac{L_2^{(1)} - L_1^{(1)}}{\varepsilon} \tag{21}$$

This implies a previous number of iterations to the optimal attenuation search, which depend on the selected precision. The interior points $L_3^{(k)}$ and $L_4^{(k)}$ (assuming that $\varphi(L_3^{(1)}) > \varphi(L_4^{(1)})$) of the kth subinterval $[L_1^{(k)}, L_2^{(k)}]$ are found using the following expressions

$$L_3^{(k)} = L_1^{(k)} + \left(1 - \frac{F_{n-k-1}}{F_{n-k}}\right)\left(L_2^{(k)} - L_1^{(k)}\right) \tag{22}$$

$$L_4^{(k)} = L_1^{(k)} + \frac{F_{n-k-1}}{F_{n-k}}\left(L_2^{(k)} - L_1^{(k)}\right) \tag{23}$$

3.2 Golden Ratio

As above, with Golden Ratio optimization algorithm [18] it is possible to replace the interval with a subinterval on which $\varphi(L)$ takes on its minimum value. One approach is to select two interior points $L_3 < L_4$. This results in $L_1 < L_2 < L_3 < L_4$. The condition that $\varphi(L)$ is unimodal guarantees that the function values $\varphi(L_3)$ and $\varphi(L_4)$ are less than $\max\{\varphi(L_1), \varphi(L_2)\}$.

If $\varphi(L_3) \leq \varphi(L_4)$, the minimum should lie in the subinterval $[L_1, L_4]$, and we replace L_2 with L_4 and continue the search in the new subinterval $[L_1, L_4]$. If $\varphi(L_4) < \varphi(L_3)$, the minimum must occur in $[L_3, L_2]$, and we replace L_1 with L_3 and continue the search in $[L_1, L_3]$.

The inner points L_3 and L_4 are selected so that the resulting intervals $[L_1, L_3]$ and $[L_4, L_2]$ are symmetrical; that is, $L_2 - L_4 = L_3 - L_1$, where

$$L_3 = L_1 + (1-r)(L_2 - L_1) = rL_1 + (1-r)L_2 \tag{24}$$

$$L_4 = L_2 - (1-r)(L_2 - L_1) = (1-r)L_1 + rL_2 \tag{25}$$

and $r = (-1 + \sqrt{5})/2$ the Golden ratio, which remains constant on each subinterval. Additionally, one of the old interior points will be used as an interior point of the new subinterval, while the other interior point will become an endpoint of the new subinterval. Thus, the number of evaluations will be two at the first iteration and then only one new point should have to be found on each iteration. The algorithm converges when the difference between $\varphi(L_2)$ and $\varphi(L_1)$ is less than the precision ϵ.

3.3 Powell

The Powell optimization algorithm [19] consists on fitting a quadratic polynomial function to known the minimum value. The method begins with an initial point (L_1), we compute $L_2 = L_1 + h$, evaluating $\varphi(L_1)$ and $\varphi(L_2)$, where h is the step size. If $\varphi(L_1) > \varphi(L_2)$ then $L_3 = L_1 + 2h$. Otherwise if $\varphi(L_1) \leq \varphi(L_2)$ then $L_3 = L_1 - h$. This process, as in the Fibonacci method, implies three previous iterations before estimating the minimum value of φ, which is defined as

$$\hat{L}_{opt} = \frac{1}{2}\frac{(L_2^2 - L_3^2)\varphi(L_1) + (L_3^2 - L_1^2)\varphi(L_2) + (L_3^2 - L_2^2)\varphi(L_3)}{(L_2 - L_3)\varphi(L_1) + (L_3 - L_1)\varphi(L_2) + (L_1 - L_2)\varphi(L_3)} \tag{26}$$

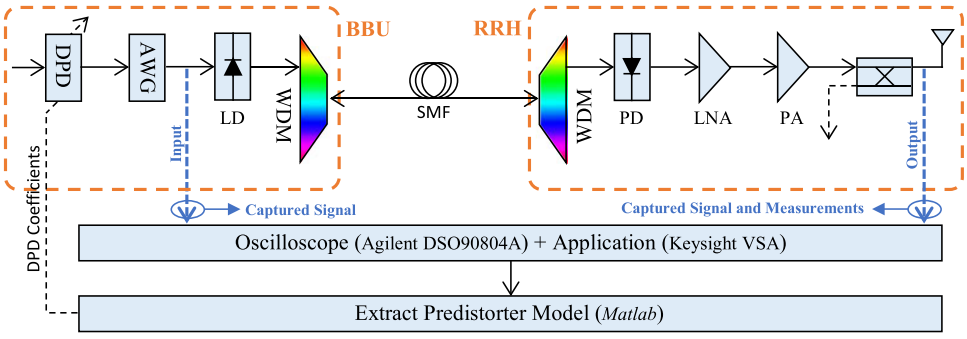

Fig. 3. Experimental setup for a RoF mobile fronthaul system without feedback loop.

If there is a lower difference between $\varphi(\hat{L}_{opt})$ and the minimum value of φ in $\{L_1, L_2, L_3\}$ than the required precision ε, the result is $\hat{L}_{opt}$. By contrast, we calculate $\varphi(\hat{L}_{opt})$ and remove the point which provides the major value for $\varphi(L)$.

In order to ensure the method convergence, the following condition has to be fulfilled

$$\frac{(L_2 - L_3)\varphi(L_1) + (L_3 - L_1)\varphi(L_2) + (L_1 - L_2)\varphi(L_3)}{(L_1 - L_2)(L_2 - L_3)(L_3 - L_1)} < 0 \tag{27}$$

4. Linearization With Ideal Feedback

4.1 Experimental Setup

The test setup used in this work is shown in Fig. 3. It consists of an IM/DD RoF system, as well as the electrical segment at the RRH. At the BBU side, an arbitrary waveform generator (AWG) (*Agilent E4438C*) is used to generate a LTE signal (OFDM modulation) with 16QAM subcarriers whose bandwidth is 20 MHz. The RF carrier frequency is set at 2.65 GHz, within the Band 7 of the LTE standard [20]. This signal is intensity modulated on an optical carrier (1550.37 nm) with an electro-absorption modulator (EAM) distributed feedback laser (DFB) (*Optilab DFB-EAM-1550-12 S/N7506*). The link between the BBU and the RRH is a single-mode fiber (SMF) with an attenuation of 0.25 dB/Km with a dispersion of 18 ps/(nm·Km). The RRH side consists of a photodetector (PD) (*Nortel Networks PP-10G*) with a responsivity of 0.9 A/W. Due to a low signal power after the optic-electric conversion, it is amplified by means of a low noise amplifier (LNA) (*Minicircuits ZX60-P33ULN+*). Then, the signal is amplified with a PA (*Minicircuits ZHL-4240*), which has a 1-dB compression point of 26 dBm, and an approximated gain of 41.7 dB at the test frequency. The wavelength-division multiplexers (WDM) and the coupler have been added to the setup in order to make a fair comparison with the following sections.

4.2 Experimental Results

The parameters for CPWL DPD identification have to be chosen carefully. Firstly we evaluate the ideal case, in which the feedback loop has not been taken into account (the output signal is captured at the RRH). The input signal power of the RoF downlink system is set at -11 dBm and -6 dBm for a fiber length of 10 and 25 km respectively, and the bias current is set at 40 mA. The model order is evaluated until $K = 10$, and the memory depths are set at $M = 0$, 1 and 2. Fig. 4 shows the performance of the DPD identification for both fiber lengths (10 and 25 km), in terms of Normalized Mean Square Error (NMSE).

Although the NMSE DPD results with the 10 km-length fiber in the setup are better than those with 25 km, when the model order increases up to 5 the model performance improves in both scenarios. Despite the larger model order and memory depth, the lower NMSE value, with model orders from $K = 5$ the DPD model gives limited performance enhancement. In terms of memory depth, when a

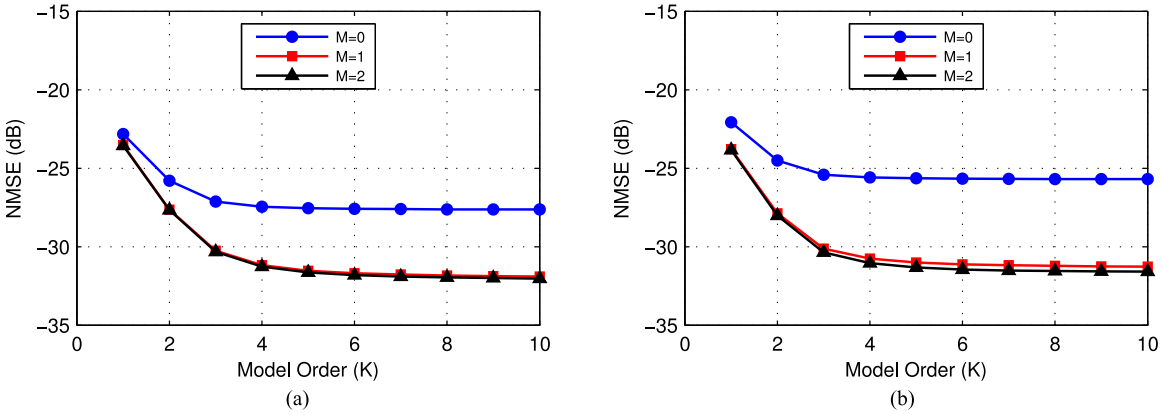

Fig. 4. Predistorter results in terms of NMSE for different model orders (K) and memory depths (M) with a fiber length of (a) 10 and (b) 25 km.

TABLE 1
Linearization Performance for the Downlink RoF System

	10 km			25 km		
Case	ACPR (dBc)	$P_{channel}$ (dBm)	EVM (%)	ACPR (dBc)	$P_{channel}$ (dBm)	EVM (%)
w/o DPD	−27.91	25.63	9.86	−27.54	25.44	10.54
DPD_{ideal}	−41.16	22.44	2.61	−40.68	22.44	2.65

tap of memory is added the NMSE decreases strongly. Instead, when the number of taps is M = 2 the model offers lightly better performance regarding to M = 1. Hence the DPD parameters are set to K = 5 and M = 1 (32 coefficients), which gives a NMSE of −31.53 and −31.00 dB for 10 and 25 km, respectively. For simplicity, these parameters are fixed for the following sections with feedback loop.

ACPR, output signal power and EVM measurements are required in order to validate the linearization performance in the downlink RoF system. According to Table 1, with the DPD in the system the ACPR improves in 13.25 and 13.14 dB in the 10 and 25 km scenarios, respectively. The linearization capacity is further confirmed by examining the output signal power spectral densities (PSD) with and without predistortion (see Fig. 5). The evaluation of the downlink RoF output power is required due to the losses introduced by the DPD, which are 3.19 and 3 dB, respectively. Finally, the EVM has been tested in order to analyze the predistorted output signal quality related to the in-band interference. Experimental results show there is an improvement of 7.25 and 7.89 percentage points with the linearization process.

5. Linearization With Feedback Loop

5.1 Experimental Setup

The experimental setup taking into account the feedback loop is shown in Fig. 6, which is similar to the previous section. The main difference lies on the feedback loop, which sends back the output signals from the RRH to the BBU. It reflects the reality of the final assembly with the need of the

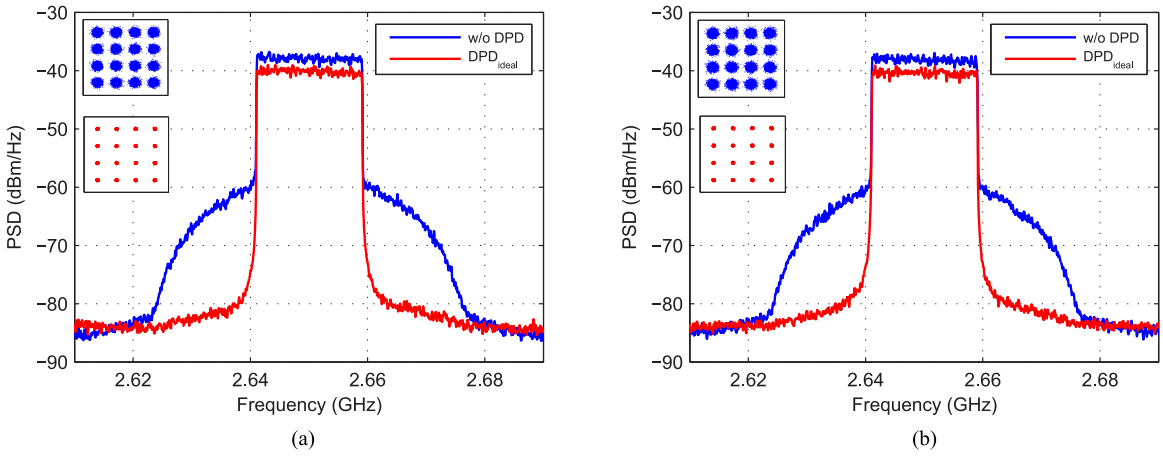

Fig. 5. Output signal PSDs and constellation diagrams without predistortion (blue) and with DPD (red) for the downlink RoF system with a fiber length of (a) 10 and (b) 25 km.

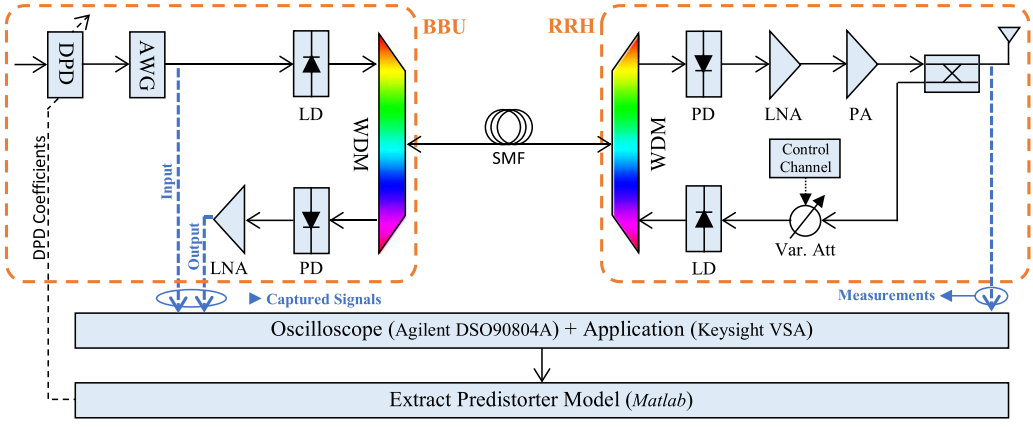

Fig. 6. Experimental setup for a RoF mobile fronthaul system with feedback loop.

feedback loop to apply the entire signal processing in the BBU. The feedback RoF link consists of an EAM-DFB (Optilab DFB-EAM-1550-12 S/N7080), which modulates in intensity the feedback signals on an optical carrier (1557.65 nm). Since the downlink and the feedback signals are directly modulated with different wavelengths it is possible to use the same fiber link with WDMs at both BBU and RRH sides. There is a PD (*Nortel Networks PP-10G*) in the BBU, which makes the optical-to-electrical conversion, and a LNA (*Minicircuits ZX60-P33ULN+*) to amplify the received signals. While in the downlink RoF system the output signal power and the power amplifier efficiency (working in its saturation region) are tried to be maximized, in the feedback RoF system the goal is to maintain the signals as linear as possible. This issue is addressed by a power alignment before the EAM-DFB located at the RRH side, which ensures the feedback RoF does not distort the signal, as discussed in Section 3.

5.2 Experimental Results

When the effects of the feedback loop are taken into account the feedback signals may suffer distortions. The output signal EVM values at the BBU side have been measured for several input signal power values in the feedback link. This task is addressed by means of a variable attenuator before the EAM-DFB located at the RRH side. In order to seek the optimum attenuation which

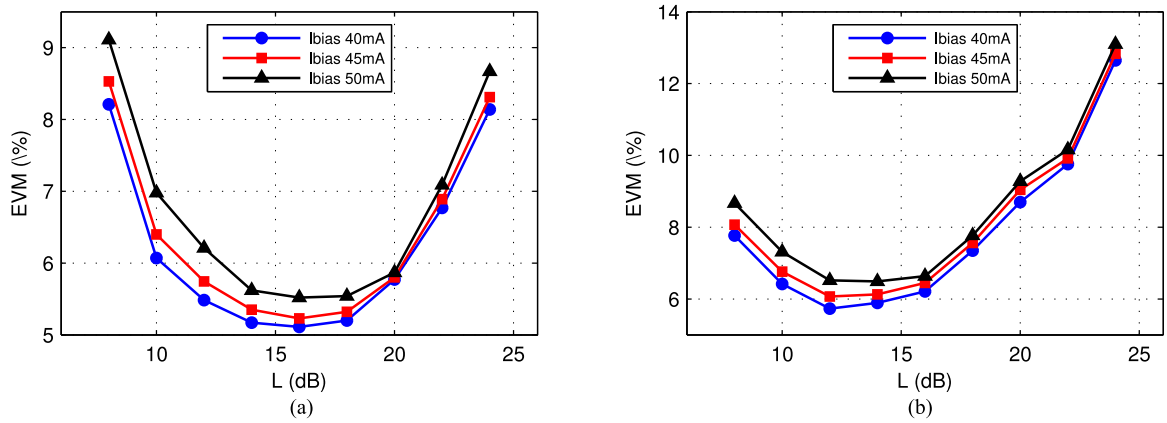

Fig. 7. EVM obtained with several attenuations in a (a) 10 and (b) 25 km-length RoF link.

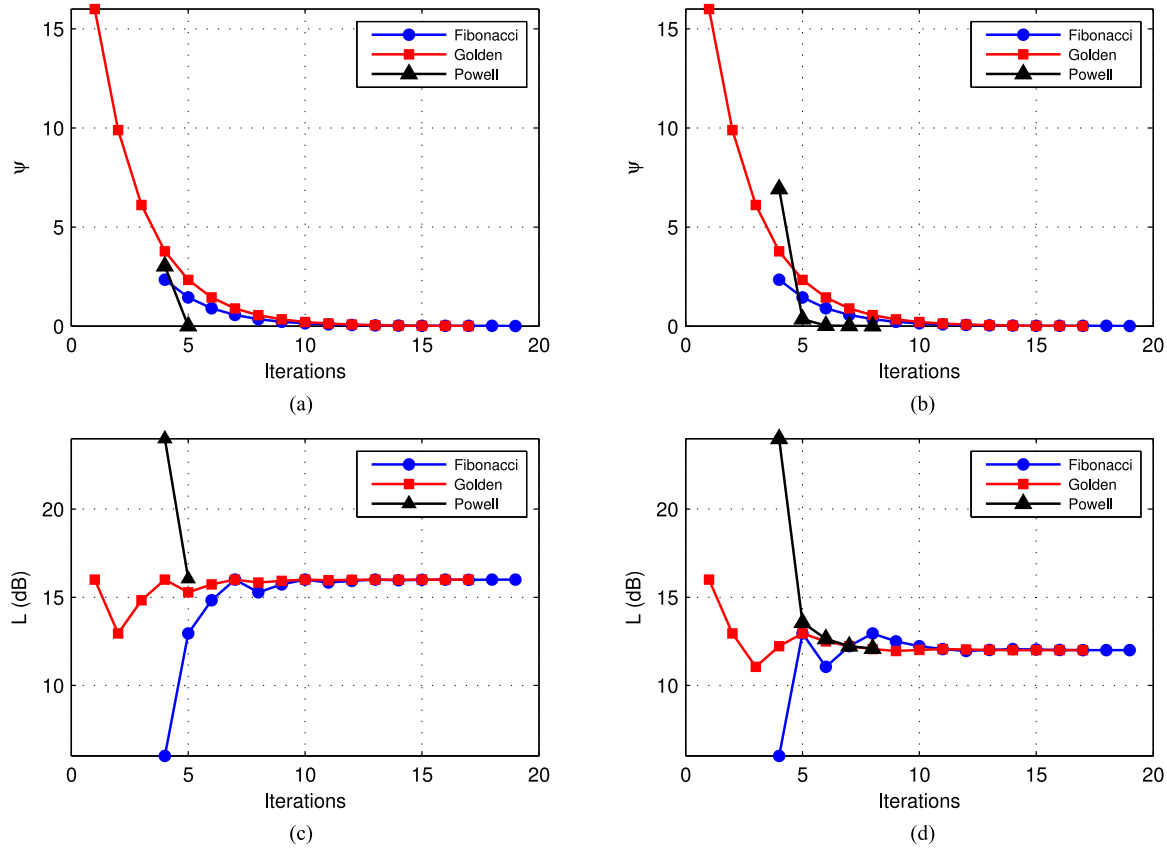

Fig. 8. Fibonacci (blue), Golden Ratio (red) and Powell (black) error convergence with a precision of 0.01 and a bias current of 40 mA with (a) 10 km-length and (b) 25 km-length; and attenuation convergence with (c) 10 km-length and (d) 25 km-length.

minimizes the feedback loop distortions, the downlink system should work in its linear region. Thus, the downlink signals are sent with a lower power than in the previous case, in particular −24 and −19 dBm, respectively. Attenuations are set between 6 and 24 dB, and the feedback loop bias current between 40 and 50 mA. In a real system the attenuator value can be remotely operated from the BBU side using a control channel. Fig. 7 shows the influence of the attenuator in the EVM of the output signals captured at the RRH side.

TABLE 2
Number of Iterations to Optimize the Feedback Attenuation With a Precision of 0.01 for Several Methods

Fiber (km)	Ibias (mA)	Fibonacci	Golden	Powell
10	40	19	17	5
	45	19	17	5
	50	19	17	5
25	40	19	17	8
	45	19	17	7
	50	19	17	5

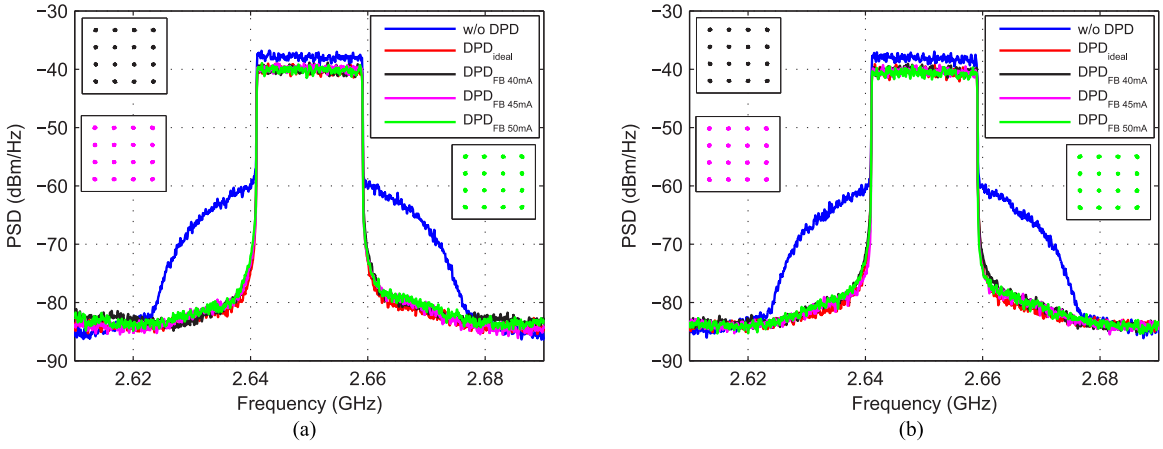

Fig. 9. Output signal PSDs and constellation diagrams without predistortion (blue), with ideal DPD (red), with feedback DPD for a bias current of 40 mA (black), 45 mA (pink) and 50 mA (green). (a) 10 km-length with an attenuation of 16 dB and (b) 25 km-length with an attenuation of 14 dB.

The higher the bias current the higher the EVM values because of the photodetector saturation. On the one hand when the attenuation is low the EVM increases because the feedback link operates in saturation region. On the other hand, when the attenuation is high the signal noise ratio decreases, producing an increment in the EVM values. If the attenuation is set properly it is possible to reach an optimum attenuation which reduces the distortion, giving a minimum value of EVM. The optimum obtained attenuator values correspond to 16 dB for all current bias in the 10 km scenario and 12 dB for 40 and 45 mA and 14 dB for 50 mA. If both setups are compared it is obvious that with 25 km-length the higher attenuations produce worse EVM values than with 10 km-length due to the losses introduced by the fiber.

Initially, the optimum attenuation is unknown, so it is necessary to seek it with as few iterations as possible. We propose the use of unconstrained optimization algorithms, commented in Section 3, such as Fibonacci, Golden or Powell, which can find the optimum attenuation value in a few iterations. The optimization algorithm error is defined as $\psi = |\varphi(L_{opt}) - \varphi(L^{(k)})|$, where $\varphi(L_{opt})$ is the optimum value and $\varphi(L^{(k)})$ is the calculated value after the k-iteration. The errors after each iteration with a precision of 0.01 and a bias current of 40 mA are shown in Fig. 8(a) and (b) with a length of 10 and 25 km, respectively. The methods end when the error (ψ) is less than the established precision (ε). Fig. 8(c) and (d) shown the mean attenuation of the interval after each iteration. As the intervals are reduced with each iteration, the attenuation converges to its optimum value. Fibonacci

TABLE 3
Linearization Performance for the Downlink RoF System With Feedback Loop

Case	10 km			25 km		
	ACPR (dBc)	$P_{channel}$ (dBm)	EVM (%)	ACPR (dBc)	$P_{channel}$ (dBm)	EVM (%)
w/o DPD	−27.91	25.63	9.86	−27.54	25.44	10.54
DPD_{ideal}	−41.16	22.44	2.61	−40.68	22.44	2.65
$DPD_{feedback\ 40\ mA}$	−40.79	22.49	2.72	−40.09	22.59	2.77
$DPD_{feedback\ 45\ mA}$	−40.58	22.42	2.77	−39.81	22.48	2.85
$DPD_{feedback\ 50\ mA}$	−40.39	22.33	2.84	−39.55	22.33	2.95

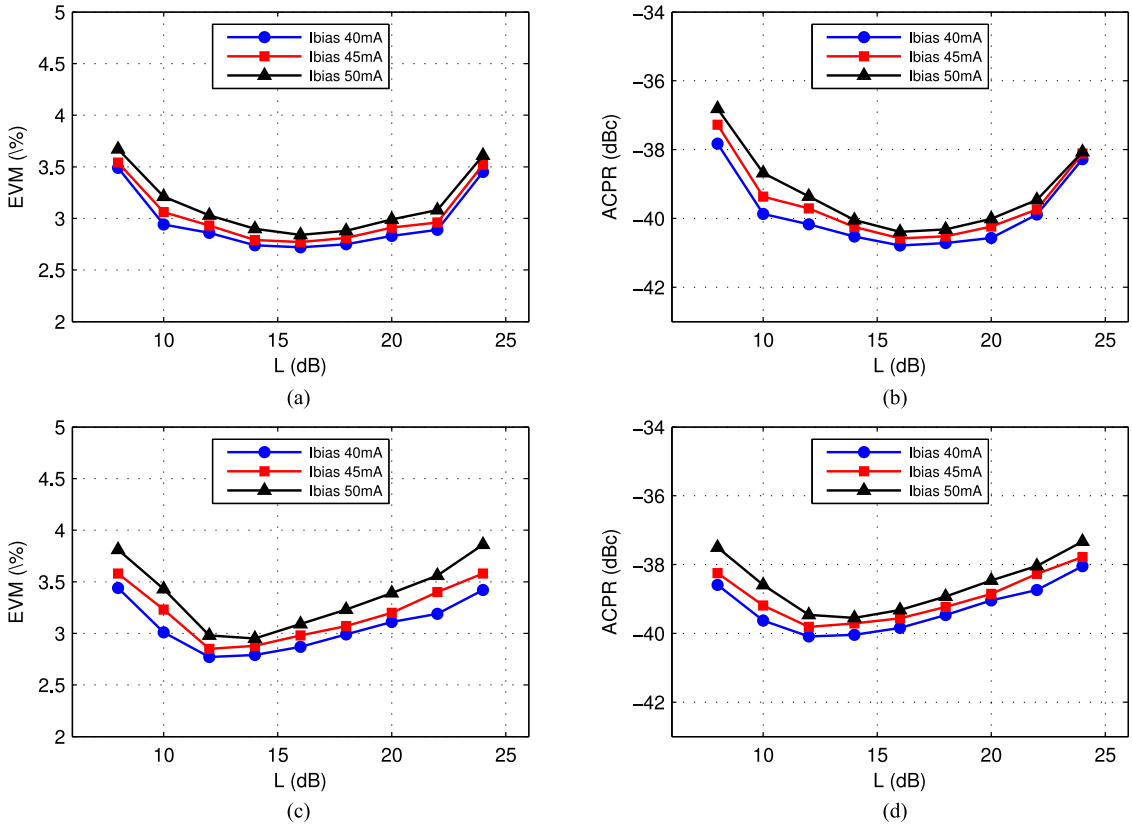

Fig. 10. Experimental results with several attenuations and bias currents with 10 km-length (a) EVM, (b) ACPR and 25 km-length (c) EVM and (d) ACPR.

algorithm needs three starting iterations in order to find the minimum value of n according to Eq. (21). This applies also to Powell method, which needs three previous iterations before estimating the optimum value. In Table 2 the iteration number for the implemented method in the different studied scenarios is gathered. Powell algorithm gives the better outcomes, since it only needs 8 iterations to converge in the worst case.

Once the optimal attenuations are known, the downlink input powers are set to the initial values (−11 and −6 dBm for 10 and 25 km-length fiber, respectively). Both the input and output signals are captured at the BBU side for linearization process with the optimal attenuation set. Once the predistorted signals are calculated, they are sent again and the experimental results are evaluated at the RRH side.

The linearization capacity is further confirmed by examining the output signal PSDs showed in Fig. 9, where the output signal power spectral densities without predistorter are plotted, with the ideal DPD calculated in the previous section and with the optimal attenuation for bias currents of 40, 45 and 50 mA in the feedback loop.

Table 3 gathers the experimental results in terms of ACPR, EVM and output signal power with the optimal attenuations. According to the ACPR measurements, with 10 km-length fiber the results are lightly better than with 25 km-length. Moreover, as in the previous section, the higher the bias current, the larger the ACPR values. These ACPR values with the optimum scenario (a bias intensity of 40 mA) are −40.79 and −40.09 dBc, close to the ideal case. Regarding the output signal power, the experimental outcomes are analogous to the ideal case. Finally, EVM decreases about 0.11 and 0.12 percentage points, respectively.

The effect of the attenuator in the linearization process performance has been evaluated. The experimental results in terms of EVM and ACPR with both scenarios are shown in Fig. 10. At the optimal attenuation, the system yields to the best performance in terms of EVM and ACPR, whereas when the attenuation increases or decreases the results get worse. The higher current bias, the worse outcomes in terms of EVM and ACPR, which agrees with the previous results.

6. Conclusion

In this work we propose the linearization of a RoF link taking into account the feedback loop in the predistortion process. While in the downlink branch we try to maximize the output power with the system working in its saturation region, in the feedback loop the goal is to minimize the distortions. In order to address this issue it is necessary to carefully choose the input power of the feedback loop by means of a variable attenuator. With the use of several optimization algorithms, such as Fibonacci, Golden and Powell, it is possible to seek the optimal attenuation with the smallest possible number of iterations. Experiments have been carried out in an IM/DD RoF system, with 10 and 25 km-length fiber, in which the feedback loop uses the same fiber link by means of several WDM at both sides of the system. Experimental results show that with a proper attenuation of the feedback signals it is possible to reach results in terms of ACPR and EVM close to the ideal case, in which the output signals are captured at the RRH.

References

[1] T. X. Vu, H. D. Nguyen, T. Q. S. Quek, and S. Sun, “Adaptive cloud radio access networks: Compression and optimization,” *IEEE Trans. Signal Process.*, vol. 65, no. 1, pp. 228–241, Jan. 2017.
[2] C. I. J. Huang, R. Duan, C. Cui, J. Jiang, and L. Li, “Recent progress on C-RAN centralization and cloudification,” *IEEE Access*, vol. 2, pp. 1030–1039, Sep. 2014.
[3] M. Peng, C. Wang, V. Lau, and H. V. Poor, “Fronthaul-constrained cloud radio access networks: Insights and challenges,” *IEEE Wireless Commun.*, vol. 22, no. 2, pp. 152–160, Apr. 2015.
[4] A. Checko *et al.*, “Cloud RAN for mobile networks-A technology overview,” *IEEE Commun. Surveys Tuts.*, vol. 17, no. 1, pp. 405–426, Jan.-Mar. 2015.
[5] Y. Xu, X. Li, J. Yu, and G. Chang, “Simple and reconfigured single-sideband OFDM RoF system,” *Opt. Exp.*, vol. 24, no. 20, pp. 22830–22835, Oct. 2016.
[6] S. E. Alavi, M. R. K. Soltanian, I. S. Amiri, M. Khalily, A. S. M. Supaat, and H. Ahmad, “Towards 5G: A photonic based millimeter wave signal generation for applying in 5G access fronthaul,” *Sci. Rep.*, vol. 6, pp. 1–11, Jan. 2016.
[7] F. Fuochi, M. U. Hadi, J. Nanni, P. A. Traverso, and G. Tartarini, “Digital predistortion technique for the compensation of nonlinear effects in radio over-fiber links,” in *Proc. IEEE 2nd. Int. Forum Res. Technol. Soc. Ind. Leveraging Better Tomorrow*, Sep. 2016, pp. 1–6.
[8] F. H. Raab *et al.*, “Power amplifiers and transmitters for RF and microwave,” *IEEE Trans. Microw. Theory Technol.*, vol. 50, no. 3, pp. 814–826, Mar. 2002.
[9] J. Amstrong, “OFDM of optical communications,” *J. Lightw. Technol.*, vol. 27, no. 3, pp. 189–204, Feb. 2009.

[10] J. Song and H. Ochiai, "Performance analysis for OFDM signals with peak cancellation," *IEEE Trans. Microw. Theory Technol.*, vol. 64, no. 1, pp. 261–270, Jan. 2016.
[11] R. Zhu, D. Shen, X. Zhang, and T. Liu, "Analysis of dual wavelength linearization technique for radio-over-fiber systems with electro-absorption modulator," *IEEE Trans. Microw. Theory Technol.*, vol. 63, no. 8, pp. 2692–2702, Aug. 2015.
[12] Y. Pei *et al.*, "Complexity-reduced digital predistortion for subcarrier multiplexed radio over fiber systems transmitting sparse multi-band RF signals," *Opt. Exp.*, vol. 21, no. 3, pp. 3708–3714, Feb. 2013.
[13] C. Han, S. Cho, H. S. Chung, and J. H. Lee, "Linearity improvement of directly-modulated multi-IF-over-fiber LTE-A mobile fronthaul link using shunt diode predistorter," in *Proc. 41st Eur. Conf. Opt. Commun.*, Sep. 2015, Paper 0781.
[14] L. O. Chua and S. M. Kang, "Section-wise piecewise-linear functions: Canonical representation, properties, and applications," *Proc. IEEE*, vol. 65, no. 6, pp. 915–929, Jun. 1977.
[15] A. Zhu, "Decomposed vector rotation-based behavioral modeling for digital predistortion of RF power amplifiers," *IEEE Trans. Microw. Theory Technol.*, vol. 63, no. 2, pp. 737–744, Feb. 2015.
[16] C. Mateo, P. L. Carro, P. García-Dúcar, J. de Mingo, and I. Salinas, "Radio-over-fiber linearization with optimized genetic algorithm CPWL model," *Opt. Exp.*, vol. 25, no. 4, pp. 3694–3708, Feb. 2017.
[17] L. Guan and A. Zhu, "Optimized low-complexity implementation of least squares based model extraction for digital predistortion of RF power amplifiers," *IEEE Trans. Microw. Theory Technol.*, vol. 60, no. 3, pp. 594–603, Mar. 2012.
[18] S. Kao-Ping, L. Yin-Feng, and Z. Ji-Cheng, "Method for optimizing the system of production well," in *Proc. Asia-Pacific Power Energy Eng. Conf.*, Mar. 2011, pp. 1–3.
[19] M. J. D. Powell, "An efficient method for finding the minimum of a function of several variables without calculating derivates," *Comput. J.*, vol. 7, no. 2, pp. 155–162, 1964.
[20] 3GPP, "Base station (BS) transmission and reception," Technical Specification ETSI TS136.104 V13.3.0, 2016.